

LOOKING FOR SPECTRAL SIGNATURES OF DIPOLAR ORDERING IN Li@C₆₀PF₆ ENDOFULLERENE

S. S. Zhukov^{a*}, *A. V. Melentev*^a, *M. Savinov*^b, *E. S. Zhukova*^a, *H. Suzuki*^c, *M. Nakano*^d,
S. Aoyagi^e, *B. P. Gorshunov*^a

^a *Moscow Center for Advanced Studies
123592, Moscow, Russia*

^b *Institute of Physics, Czech Academy of Sciences
18221, Praha 8, Czech Republic*

^c *Department of Chemistry, Kindai University
577-8502, Osaka, Japan*

^d *Research Center for Thermal and Entropic Science,
Graduate School of Science, Osaka University
560-0043, Osaka, Japan*

^e *Department of Information and Basic Science,
Nagoya City University
467-8501, Nagoya, Japan*

Received October 10, 2024,
revised version October 10, 2024,
Accepted for publication October 15, 2024

Using terahertz (THz) and radio-frequency (RF) spectroscopy, spectra of the complex dielectric permittivity $\varepsilon^*(\nu) = \varepsilon'(\nu) + i\varepsilon''(\nu)$ of pressed pellets of metallofullerene ${}^6\text{Li}@\text{C}_{60}\text{PF}_6$ are measured in the frequency ranges $\nu = 0.3\text{--}3\text{ THz}$ ($10\text{--}110\text{ cm}^{-1}$) ($T = 5\text{--}300\text{ K}$) and $1\text{ Hz--}1\text{ MHz}$ ($T = 0.3\text{--}60\text{ K}$). In the THz region, a temperature-unstable absorption band is observed and two possible interpretations of its origin are presented, based either on the quantized rotation of the Li ion within the C₆₀ cage or on the hopping of Li over minima in the multi-well localizing potential. A pronounced maximum in the temperature dependence of the real RF permittivity $\varepsilon'(T)$ is observed at around the temperature $T_C = 24\text{ K}$ of a previously discovered phase transition of presumably antiferroelectric type. The maximum is attributed to the temperature evolution of a soft relaxation band lying outside our working frequency intervals — at $1\text{ MHz} < \nu < 0.3\text{ THz}$. It is shown that the frequency of this band has a V-shaped temperature dependence around the transition temperature T_C and that it does not vanish at T_C , both features typically observed for the ferroelectric order-disorder phase transitions. It is concluded that dielectric measurements of Li@C₆₀PF₆ in the microwave frequency range are required in order to obtain detailed information on the parameters and on the temperature behavior of the soft relaxation, which will provide information on the microscopic origin of the phase transition.

DOI: 10.31857/S0044451025030022

1. INTRODUCTION

Endofullerenes provide a unique playground for the studies of materials properties in condition of nanoconfinement. The state of the nano-confined atom or molecule, or their conglomerates, can be largely determined by quantum effects, making it possible to

study, e.g., the nature of the interconversion of molecular ortho- and para- spin isomers [1, 2], energy states of quantized rotational and vibrational molecular motion, possibilities of realizing quantum entanglement states [3], etc. In addition, coupling between trapped molecules possessing electric or magnetic moments can lead to a variety of collective effects, such as electric and magnetic ordering or quantum critical phenomena [4–8]. The existence of such a diverse range of physical properties of endofullerenes is a source of interest

* E-mail: ssz1978@gmail.com

with regard to their widespread range of potential applications in biomedicine, molecular electronics, photonics, etc. It can be posited that the attractiveness of a specific system, in both fundamental and practical aspects, is to some extent contingent upon by the diversity of the possible energy states it is capable of attaining. In this respect, the metallofullerene $\text{Li}^+\text{@C}_{60}\text{PF}_6^-$ is especially attractive. With a variety of localized states of the relatively small Li^+ ion can occupy within the C_{60} cage (theory predicts 20 local positions of Li^+ within C_{60} [9]), with the possibility of tunneling between these states [10], together with the charge transfer from Li@C_{60} to PF_6 creating large (up to ≈ 20 Debye [11]) electric dipole moments that strongly interact with each other, the compound exhibits a rich palette of exciting physical properties that are being actively considered for use in the creation of molecular multistage switches [12, 13], qubits [10], hydrogen storage materials [14], elements for optical high harmonic generation [15], etc.

Electrostatic coupling between Li^+ ions and PF_6^- molecules was found to be at the origin of a phase transition in $\text{Li@C}_{60}\text{PF}_6$ taking place at around 24 K, leading to an anomaly of specific heat and a peak in dielectric constant at this temperature [10, 16]. XRD experiments on single-crystalline $\text{Li@C}_{60}\text{PF}_6$ did not reveal any structural changes of the crystal lattice, so that the transition was associated with the partial ordering during cooling of Li^+ ions inside C_{60} . It was also assumed that the phase transition is of a second- or higher order type, and a possible explanation was suggested that the transition could be connected with an antiferroelectric ordering of the dipoles formed by caged Li^+ and PF_6^- molecules outside the C_{60} cages. However, no further attempts have been made to study the transition in more detail. The goal of the present study is to gain a deeper insight into the microscopic origin of this phase transition by using terahertz and radio-frequency spectroscopies. These techniques have proved to be among the most effective tools used to study the mechanisms of structural, order-disorder or mixed type phase transitions in dipolar ordered systems by exploring the behavior of the soft excitations (phonon or relaxational in origin) subject to external stimuli — temperature, pressure, strain, electric or magnetic external fields, etc. (see [17, 18] and references therein). In the case of a displacive ferroelectric (FE) phase transitions, one observes a Curie–Weiss increase during cooling of the quasi-static dielectric constant which is caused by softening (i. e., decrease in frequency position ν_0) of one of the phonon transverse polar modes (the soft mode) ac-

cording to the Cochran law, $\nu_0 \sim (T - T_C)^{0.5}$ (T_C is the transition temperature)[19]. In the case of an order-disorder phase transition, the role of the soft mode is played by a soft relaxation whose peak frequency changes linearly with the temperature, $\nu_0 \sim T - T_C$ [20]. It should be noted that many ferroelectric compounds exhibit features characteristic of both types [21, 22].

In [10], a Curie–Weiss temperature dependence of the dielectric constant of $^7\text{Li@C}_{60}\text{PF}_6$ single crystals above the phase transition temperature of 24 K was observed. However, so far, no information is available on the soft mode that could be associated with the transition. A temperature-unstable terahertz absorption band observed in the $^7\text{Li@C}_{60}\text{PF}_6$ crystal in [23] was interpreted based on the consideration of the quantized rotation of the Li ion within the C_{60} cage, rather than with the FE soft mode. In the search for such a soft mode in $\text{Li@C}_{60}\text{PF}_6$, which can provide with the new detailed information on the nature of the 24 K phase transition, we have performed terahertz (THz) and radio-frequency (RF) measurements of the dielectric response of $^6\text{Li@C}_{60}\text{PF}_6$ at temperatures ranging from 300 K to 5 K (THz) and from 300 K to 0.3 K (RF).

2. EXPERIMENTAL DETAILS

The $^6\text{Li@C}_{60}\text{PF}_6$ powder sample was prepared at Idea International Co. Ltd. by the plasma method [24, 25] of preparing $^7\text{Li@C}_{60}\text{PF}_6$ except that ^6Li ions with the 95% isotopic purity were irradiated to C_{60} . For THz and RF measurements, pellets with a thickness 100–200 μm and a diameter of 8 mm were prepared by pressing. For THz measurements in the frequency range $\nu = 0.3\text{--}3\text{ THz}$ ($10\text{--}110\text{ cm}^{-1}$), a time-domain TeraView 3000 spectrometer was employed to directly determine the spectra of the real $\varepsilon'(\nu)$ and imaginary $\varepsilon''(\nu)$ parts of the complex dielectric permittivity $\varepsilon^*(\nu) = \varepsilon'(\nu) + i\varepsilon''(\nu)$ from the complex (amplitude and phase) transmission coefficient spectra of the pellets. RF measurements at frequencies 1 Hz–1 MHz were done in vacuum using a NOVOCONTROL Alpha AN High Performance Frequency Analyzer equipped with an additional ^3He system (Cryogenic Limited), capable of controlling temperature from 300 K down to 0.3 K. Pt–Au-electrodes (diameter 5 mm) were evaporated using a Bal-Tex SCD 050 sputter coater onto the faces of the pellets. The contacts for applying the AC electric field were provided by silver wires fixed to the electrodes by a silver paste.

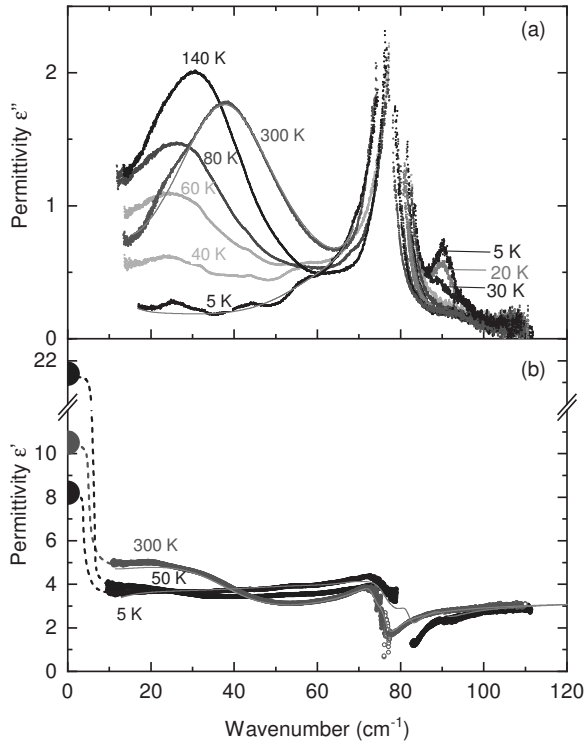


Fig. 1. Terahertz spectra of the imaginary $\varepsilon''(\nu)$ (a) and real $\varepsilon'(\nu)$ (b) parts of the dielectric permittivity of a pressed pellet of ${}^6\text{Li}@\text{C}_{60}\text{PF}_6$ measured at different temperatures. The solid lines show least-square fits of the spectra measured at 5 K and 300 K with the Lorentzian expression (1). The weak wavy structure seen in the $\varepsilon''(\nu)$ spectra at 5 K and 40 K is caused by interferometric resonances of radiation within the plane-parallel pellet (Fabry–Perot effect). The dashed lines in panel (b) show extrapolations of the $\varepsilon'(\nu)$ spectra to the radio-frequency permittivity data (thick dots) measured at 0.95 MHz. The significantly larger RF permittivity compared to the THz permittivity clearly indicates the presence of an excitation in the microwave frequency range, as discussed in the text

3. RESULTS AND DISCUSSION

Figure 1 shows THz spectra of imaginary and real permittivities measured at several temperatures. Relatively narrow resonances are observed around $70\text{--}80\text{ cm}^{-1}$ whose origin can be associated with the transverse phonons of the rock-salt type crystal lattice of $\text{Li}@\text{C}_{60}\text{PF}_6$ [23, 26]. At lower frequencies, we observe an absorption band whose frequency decreases from 40 cm^{-1} at 300 K to 30 cm^{-1} at 5 K. However, the band cannot be associated with the ferroelectric soft mode, because its intensity decreases strongly on cooling, in contrast to the FE soft mode. In [23], the band was explained by considering the quantum rotation of the Li ion over a spherical shell inside the C_{60}

cage. Such rotation produces a series of narrow energy levels whose envelope reproduces the measured spectrum quite well. The freezing out of the band on cooling was attributed to the decrease in the energy levels population governed by the Boltzmann factor. Another interpretation of the THz band can also be suggested. The least-square fitting of the spectra shown in Fig. 1 with the Lorentzian expression for the complex dielectric permittivity

$$\varepsilon^*(\nu) = \frac{\Delta\varepsilon \nu_0^2}{\nu_0^2 - \nu^2 - i\nu\gamma} \quad (1)$$

allowed us to obtain the temperature dependence of the band parameters: the frequency position ν_0 , the dielectric contribution $\Delta\varepsilon$, the oscillator strength $f = \Delta\varepsilon \nu_0^2$, and the damping parameter γ . The Arrhenius plots of the frequency and the oscillator strength of the band are shown in Fig. 2. It can be seen that at $T = 120\text{--}300\text{ K}$, the temperature change of the band frequency follows the expression $\nu_0 = A \exp(-E_{\text{act}}/k_B T)$ with the activation energy $E_{\text{act}} = 3.9\text{ meV}$, which is a signature of the relaxational dielectric response [27] (k_B is the Boltzmann constant).

This allows us to suggest that the band can be associated with the thermally activated hopping of Li ions over 20 potential minima of the localizing potential [9, 28, 29]. The weakening of the activated behavior below $\approx 120\text{ K}$ with a subsequent transition to a temperature-independent regime below 60 K can be explained by a switching of the temperature-activated hopping regime to the tunnel-assisted hopping regime [10]. From Fig. 2b it can be seen that during cooling from 300 K to $\approx 30\text{ K}$, the oscillator strength of the band decreases in an activated manner with $E_{\text{act}} = 4.3\text{ meV}$ ($T > 100\text{ K}$) and $E_{\text{act}} = 7\text{ meV}$ ($T < 100\text{ K}$). This decrease can be attributed to the depletion of the amount of hopping Li ions due to their condensation into two equivalent potential minima close to hexagons in the C_{60} cage [10, 29]. The determined values of the activation energy can be associated with the depth of the potential well experienced by the Li ions: $E_{\text{act}} = 4.3\text{ meV}$ at $T > 100\text{ K}$ and $E_{\text{act}} = 7\text{ meV}$ at $T < 100\text{ K}$.

We now turn to the lower-frequency dielectric response of the material that is represented by the RF spectra of the real and imaginary permittivities in Fig. 3. We will consider the spectra measured at temperatures below 60 K, i.e., in the temperature interval where the 24 K phase transition was observed. In the $\varepsilon''(\nu)$ spectra two relaxational bands can be distinguished whose peak frequencies monotonically decrease with cooling. Signs of relaxational response in

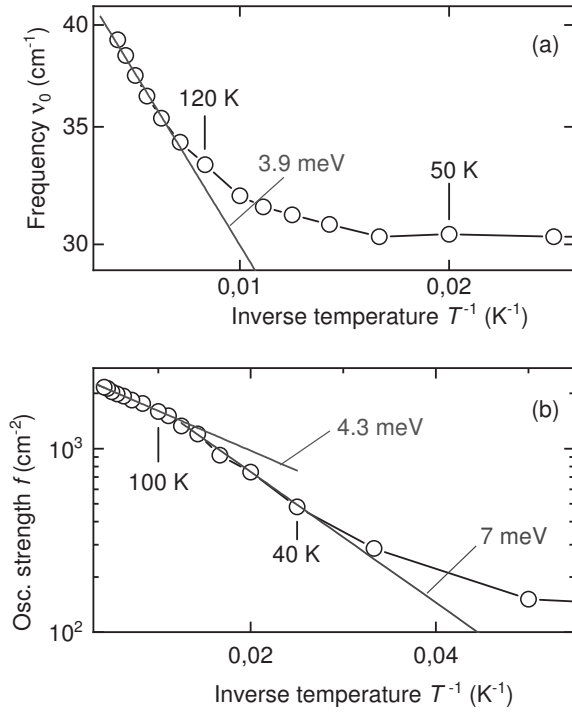


Fig. 2. Arrhenius plots of the temperature dependence of the frequency position (a) and oscillator strength (b) of the terahertz temperature-dependent excitation found below 60 cm^{-1} in ${}^6\text{Li@C}_{60}\text{PF}_6$ (Fig. 1 a). Straight lines represent activation behavior with activation energies as indicated. Vertical bars mark specific temperatures

the form of frequency-dependent imaginary permittivity were also detected earlier [10] in the RF experiments performed on the $\text{Li@C}_{60}\text{PF}_6$ single crystals. Signatures of the two relaxations are seen as peaks around 12 K and 46 K in the temperature dependence of the imaginary permittivity $\varepsilon''(T)$ measured at $\approx 1 \text{ MHz}$ represented by blue dots in Fig. 4. There is one more peak in the $\varepsilon''(T)$ dependence at 30 K, but the corresponding relaxation band is not visible in the spectra in Fig. 3 a, probably due to its relatively low intensity on the background of strong growth of $\varepsilon''(\nu)$ above 10^5 Hz . Let us refer to the earlier measurements of the RF $\varepsilon'(\nu)$ and $\varepsilon''(\nu)$ spectra of polar water molecules located within nano-voids of the cordierite crystal lattice [30]. These experiments allowed us to discover a phase transition at $T_0 = 2 \text{ K}$ from the paraelectric phase with disordered H_2O dipoles to the phase with a mixed ferroelectric-antiferroelectric type of the dipolar ordering. The key finding in this work was the observation of a relaxation band whose peak frequency ν_{peak} decreases and then increases during cooling, thus displaying a V-shaped $\nu_{\text{peak}}(T)$ dependence around the transition temperature $T_0 = 2 \text{ K}$. No such

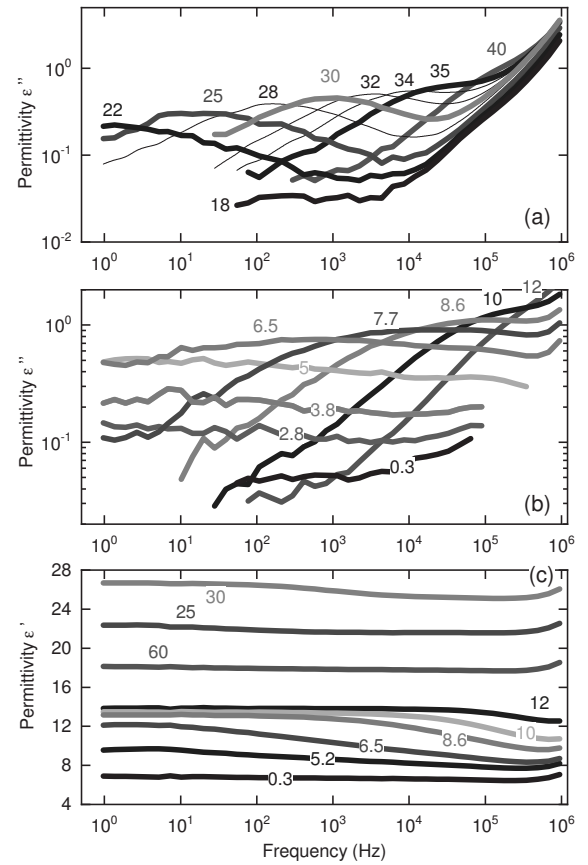


Fig. 3. Radio-frequency spectra of the imaginary $\varepsilon''(\nu)$ (a,b) and real $\varepsilon'(\nu)$ (c) parts of the dielectric permittivity of a pressed pellet of ${}^6\text{Li@C}_{60}\text{PF}_6$. Numbers indicate measurement temperatures in degrees K

behavior of the relaxations can be revealed in the spectra of ${}^6\text{Li@C}_{60}\text{PF}_6$.

The observed relaxational bands are relatively weak, as can be seen in Fig. 3 c, where the values of their dielectric contributions $\Delta\varepsilon \leq 3$ correspond to the amplitudes of the «steps» in the $\varepsilon'(\nu)$ spectra, i. e., to the difference between the low and high frequency permittivity $\varepsilon'(\nu)$. According to Fig. 4, the overall change in the real permittivity during the temperature variation is about 20, i. e., significantly larger. We assume that the origin of the observed relaxations is related to the granular nature of the samples. To clarify this point, RF measurements on single crystalline $\text{Li@C}_{60}\text{PF}_6$ are in progress.

Significantly lower values of the THz real permittivity $\varepsilon'(10 \text{ cm}^{-1})$ (open red dots in Fig. 4) compared to the RF permittivity $\varepsilon'(0.95 \text{ MHz})$ (closed blue dots in Fig. 4), see also Fig. 1 b, together with the nearly dispersionless RF spectra of $\varepsilon'(\nu)$ below 1 MHz (Fig. 3 c)

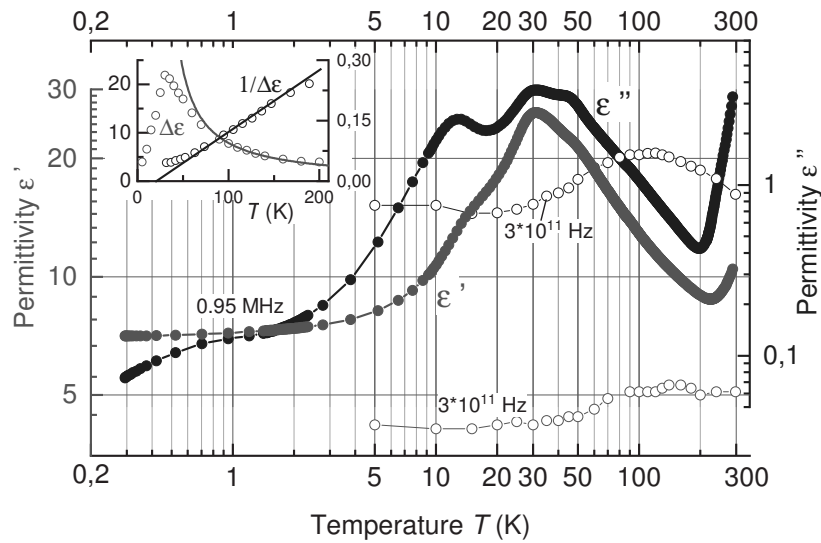


Fig. 4. Temperature dependence of the real $\varepsilon'(\nu)$ and imaginary $\varepsilon''(\nu)$ parts of the dielectric permittivity of a pressed pellet of ${}^6\text{Li}@\text{C}_{60}\text{PF}_6$ measured at 0.95 MHz (full dots) and 0.3 THz (10 cm^{-1} , open dots). Strong increase of the RF $\varepsilon'(\nu)$ and $\varepsilon''(\nu)$ values above $\approx 200\text{ K}$ can be connected with the excitation accompanying the structural phase transition at $\approx 360\text{ K}$ [16]. Inset shows the Curie–Weiss temperature dependence of the dielectric contribution $\Delta\varepsilon$ and inverse $\Delta\varepsilon^{-1}$ of the excitation located between 1 MHz and 0.3 THz (10 cm^{-1}) determined as $\Delta\varepsilon = \varepsilon'(1\text{ MHz}) - \varepsilon'(0.3\text{ THz})$: $\Delta\varepsilon = C(T - T_C)^{-1}$ with the Curie constant $C = 600\text{ K}$ and $T_C = 24\text{ K}$ (red and blue lines)

clearly indicate the presence of a strong excitation located in the microwave range, between 1 MHz and 0.3 THz (10 cm^{-1}). We believe that it is this excitation that should be associated with the phase transition observed at 24 K. As was mentioned above, the transition does not affect the crystal symmetry, but is associated with the temperature-dependent spatial positioning of the Li ions which experience a multi-well localizing potential within the C_{60} cages. This suggests that the phase transition is of the order-disorder type. Then the peak observed at about 30 K in the RF permittivity $\varepsilon'(T)$ should be mainly related to the temperature evolution of the soft relaxation located at microwave frequencies. Its dielectric contribution determined as $\Delta\varepsilon = \varepsilon'(1\text{ MHz}) - \varepsilon'(0.3\text{ THz})$ is well described by the Curie–Weiss expression $\Delta\varepsilon = C(T - T_C)^{-1}$ in the range $T = 100\text{--}200\text{ K}$ (red line in the inset of Fig. 4), with the transition temperature $T_C = 24\text{ K}$ and with the Curie constant $C = 600\text{ K}$, the value that is typical for the order-disorder type transitions in ferroelectrics [20]. Similar Curie–Weiss-like temperature dependence $\varepsilon'(T)$ was also observed in the ${}^7\text{Li}@\text{C}_{60}\text{PF}_6$ single crystal [10].

We can propose the following scenario. During cooling below 200 K, the microwave soft relaxation is essentially the spectral response associated with the anharmonic thermal hopping of the Li ions over 20 local

minima within the C_{60} cage. The peak position ν_0 of the relaxation decreases and the dielectric contribution $\Delta\varepsilon$ grows following the Curie–Weiss dependence (inset in Fig. 4). Below $\approx 100\text{ K}$, deviations from the Curie–Weiss behavior of the dielectric contribution are observed because the Li ions begin to condense within the two equivalent minima, which arise due to the polar $\text{Li}^+ - \text{PF}_6^-$ interaction through the C_{60} cage [10, 29]. Below 24 K, these minima become non-equivalent due to the collective interaction of the dipoles formed by positive Li^+ and negative PF_6^- , which order antiferroelectrically below this temperature [10, 16]. This process is accompanied by a decrease in the soft relaxation frequency ν_0 as $T_C = 24\text{ K}$ is approached and its subsequent increase on further cooling. The peak frequency ν_0 does not reach zero value, but shows a V-shaped $\nu_0(T)$ dependence with a minimum at T_C and with the minimum value lying above 1 MHz. The described $\Delta\varepsilon(T)$ and $\nu_0(T)$ behaviors are typically observed in the order-disorder ferroelectrics [22, 31, 32]. In order to gain a deeper insight into the microscopic processes that are at the origin of the phase transition in $\text{Li}@\text{C}_{60}\text{PF}_6$ measurements in the microwave frequency range are required which will provide more information on the temperature evolution and the parameters of the soft relaxation.

4. CONCLUSIONS

In the terahertz region $\nu = 10\text{--}110\text{ cm}^{-1}$, a temperature-unstable absorption band is observed in the real $\varepsilon'(\nu)$ and imaginary $\varepsilon''(\nu)$ permittivity spectra of the pressed pellet of ${}^6\text{Li}@C_{60}\text{PF}_6$ endofullerene. The band cannot be considered as a ferroelectric soft mode associated with the phase transition at $T_C = 24\text{ K}$. Its origin can be explained by considering the quantized rotation of the Li ion within the C_{60} cage, or by the hopping of Li over minima in the multi-well localizing potential. The soft relaxation which is associated with the phase transition is located at $\nu > 1\text{ MHz}$, i. e., above our radiofrequency working interval of $1\text{ Hz--}1\text{ MHz}$. A pronounced maximum in the temperature dependence of the real permittivity $\varepsilon'(1\text{ MHz})$ observed at around T_C is caused by the temperature evolution of the soft relaxation, which shows a V-shaped temperature dependence of the peak frequency around T_C , as typically observed for the ferroelectric order-disorder phase transitions. The dielectric measurements of $\text{Li}@C_{60}\text{PF}_6$ in the microwave frequency range are required in order to obtain detailed information on the parameters and on the temperature behavior of the soft relaxation, which will provide information on the microscopic origin of the phase transition.

Acknowledgements. We wish to thank for P. Proschek and J. Prokleska for their assistance with the radio-frequency experiments and N. Orekhov, M. V. Talanov, M. Sajadi and A. Chernov for fruitful discussions.

Funding. The work was supported by the Russian Science Foundation grant № 23-22-00105.

REFERENCES

1. B. Meier, S. Mamone, M. Concistrè, et al., Nat. Commun. **6**, 8112 (2015).
2. S. Mamone, M. R. Johnson, J. Ollivier, et al., Phys Chem Chem Phys **18**, 1998 (2016).
3. S. Sitha, J. Mol. Model. **29**, 242 (2023).
4. A. Krachmalnicoff, R. Bounds, S. Mamone, et al., Nat. Chem. **8**, 953 (2016).
5. Y. Zhao, Y. Guo, Y. Qi, et al., Adv. Sci. **10**, 2301265 (2023).
6. T. Serwatka, P.-N. Roy, J. Phys. Chem. Lett. **14**, 5586 (2023).
7. T. Serwatka, P.-N. Roy, J. Chem. Phys. **160**, 104302 (2024).
8. Y. Shen, M. Cui, S. Takaishi et al., Nat Commun. **13**, 495 (2022).
9. M. Zhang, L. B. Harding, S. K. Gray, S. A. Rice, J. Phys. Chem. A **112**, 5478 (2008).
10. S. Aoyagi, A. Tokumitsu, K. Sugimoto, et al., J. Phys. Soc. Jpn. **85**, 094605 (2016).
11. A. K. Srivastava, A. Kumar, N. Misra, Phys. E Low-Dimens. Syst. Nanostructures **84**, 524 (2016).
12. H. J. Chandler, M. Stefanou, E. E. B. Campbell, R. Schaub, Nat. Commun. **10**, 2283 (2019).
13. A. K. Ismael, ACS Omega **8**, 19767 (2023).
14. Q. Wang, P. Jena, J. Phys. Chem. Lett. **3**, 1084 (2012).
15. M. Wolf, S. Toyouchi, P. Walke, et al., RSC Adv. **12**, 389 (2022).
16. H. Suzuki, M. Ishida, C. Otani, et al., Phys. Chem. Chem. Phys. **21**, 16147 (2019).
17. J. Petzelt, S. Kamba, Ferroelectrics **503**, 19 (2016).
18. S. Kamba, APL Mater. **9**, 020704 (2021).
19. W. Cochran, Phys. Rev. Lett. **3**, 412 (1959).
20. M. E. Lines, A. M. Glass, *Principles and Applications of Ferroelectrics and Related Materials*, Oxford University Press, Oxford (2001).
21. A. Bussmann-Holder, H. Beige, G. Völkel, Phys. Rev. B **79**, 184111 (2009).
22. J. Hlinka, T. Ostapchuk, D. Nuzhnyy, et al., Phys. Rev. Lett. **101**, 167402 (2008).
23. H. Suzuki, M. Ishida, M. Yamashita, et al., Phys. Chem. Chem. Phys. **18**, 31384 (2016).
24. H. Okada, Y. Matsuo, Fuller. Nanotub. Carbon Nanostructures **22**, 262 (2014).
25. S. Aoyagi, K. Miwa, H. Ueno, et al., R. Soc. Open Sci. **5**, 180337 (2018).

26. J. Hernández-Rojas, J. Bretón, J. M. Gomez Llorente, Chem. Phys. Lett. **237**, 115 (1995).
27. A. K. Jonscher, J. Phys. Appl. Phys. **32**, R57 (1999).
28. Y. Matsuo, H. Okada, H. Ueno, *Endohedral Lithium-Containing Fullerenes*, Springer Singapore, Singapore (2017).
29. S. Aoyagi, Y. Sado, E. Nishibori, et al., Angew. Chem. Int. Ed. **51**, 3377 (2012).
30. M. A. Belyanchikov, M. Savinov, Z. V. Bedran, et al., Nat. Commun. **11**, 3927 (2020).
31. J. Petzelt, G. V. Kozlov, A. A. Volkov, Ferroelectrics **73**, 101 (1987).
32. Y. Onodera, J. Phys. Soc. Jpn. **73**, 1216 (2004).